ELSEVIER

Chemical Engineering Journal 87 (2002) 261–271

Chemical Engineering Journal

www.elsevier.com/locate/cej

A synergistic effect of photocatalysis and ozonation on decomposition of formic acid in an aqueous solution

Shinpon Wang [a], Fumihide Shiraishi [a,*], Katsuyuki Nakano [b]

[a] *Faculty of Computer Science and Systems Engineering, Department of Biochemical Engineering and Science, Kyushu Institute of Technology, 680-4 Kawazu, Iizuka 820-8502, Japan*

[b] *Department of Chemical Engineering, Fukuoka University, Nanakuma, Fukuoka 814-0180, Japan*

Accepted 4 February 2002

Abstract

A synergistic effect of photocatalysis and ozonation on the decomposition of formic acid dissolving in an aqueous solution has been studied. In the photocatalysis over a thin film of titanium oxide immobilized on the inner surface of a glass tube, a 6 W blacklight blue fluorescent lamp (wavelength: 300–400 nm) was used as a light source. The initial decomposition rates followed a Langmuir–Hinshelwood type and the hydrogen peroxide generated during the photocatalytic reaction played an important role in the decomposition of formic acid. In the ozonation, a 6 W low-pressure mercury lamp (wavelength: 185 nm) was used to produce ozone by irradiation of the air with UV. When this air was circulated in a closed system with a water-holding glass container, the ozone concentrations in the air and water reached 0.350 g m^{-3} air and 0.037 g m^{-3} liquid, respectively, at maximum. The decomposition rate of formic acid by ozone was higher for a lower liquid temperature and a higher pH value. For comparison, the Langmuir–Hinshelwood type was also used to analyze both the experimental values obtained in the ozonation alone and in the combination of photocatalysis and ozonation. A relationship between the reaction rate and reactant concentration was calculated using the kinetic parameters determined from the experimental values in each reaction system. As a result, the decomposition rate of formic acid by the combination of photocatalysis and ozonation was found to be 31% higher at maximum than the sum of the decomposition rates when formic acid was individually decomposed by the two methods, which indicates the presence of a synergistic effect of the photocatalysis and ozonation. This effect may be explained by the promoted production of hydroxyl radicals by ozone over titanium oxide. © 2002 Elsevier Science B.V. All rights reserved.

Keywords: Photocatalysis; Ozonation; Formic acid; Synergistic effect; Langmuir–Hinshelwood type

1. Introduction

For the treatment of wastewaters that contain trace recalcitrant organic compounds, such as organo-halogens, organic pesticides, surfactants, and coloring matters, water engineers are now required to develop advanced treatment processes. In general, a combination of several methods gives high treatment efficiency compared with individual treatment. For example, a certain organic compound can hardly be degraded by ozonation or photolysis alone and the treated wastewater may be more dangerous as a result of ozonation [1–4], but a combination of several treatment methods, such as O_3/VUV, O_3/H_2O_2/UV, and UV/H_2O_2, improves the removal of pollutants from the wastewater [5–7].

On the other hand, photocatalysis has a great potential for the removal of organic pollutants from wastewaters [8,9], although it is not still in practical use because of its low oxidation rate. Therefore, a combination of photocatalyst with the ozone that is a strong oxidizer is reasonable for the treatment of hardly degradable organic compounds since the organic compounds are expected to decompose more quickly and thoroughly to the level of carbon dioxide, water, or inorganic ions. Sanchez et al. [10] combined these two methods for the removal of aniline from water and found that the decomposition rate of aniline is larger than when individually treated by these methods. Since aniline is a relatively large molecular-weight compound, however, there were many unidentified intermediates affecting the decomposition rate. Consequently, they did not kinetically analyze the combined effect of photocatalysis and ozonation.

In the present work, a synergistic effect of photocatalysis and ozonation is studied using formic acid of a simpler structure as a reactant. A 6 W blacklight blue fluorescent lamp (wavelength: 300–400 nm) is used to excite the photocatalyst surface, while a 6 W low-pressure mercury lamp (wavelength: 185 nm) is used to produce ozone by irradiating the air. Three types of operations (photocatalysis, ozonation,

* Corresponding author. Tel.: +81-948-29-7827; fax: +81-948-29-7801.
E-mail address: fumi@bse.kyutech.ac.jp (F. Shiraishi).

1385-8947/02/$ – see front matter © 2002 Elsevier Science B.V. All rights reserved.
PII: S1385-8947(02)00016-5

Nomenclature

C	reactant concentration ($g\,m^{-3}$)
C_0	initial reactant concentration ($g\,m^{-3}$)
k	kinetic constant ($g\,m^{-3}\,min^{-1}$)
k^{app}	apparent kinetic constant ($g\,m^{-3}\,min^{-1}$)
K_H	adsorption equilibrium constant ($m^3\,g^{-1}$)
K_H^{app}	apparent adsorption equilibrium constant ($m^3\,g^{-1}$)
r	decomposition rate ($g\,m^{-3}\,min^{-1}$)
r_0	initial decomposition rate ($g\,m^{-3}\,min^{-1}$)
t	time (min)

and combination of these two methods) are investigated in a batch-recirculation manner. For comparison, the experimental values obtained in each operation are kinetically analyzed in terms of a Langmuir–Hinshelwood type.

2. Experimental

2.1. Chemicals and materials

All chemicals (at least, of reagent grade) were purchased from Wako Pure Chemicals (Osaka, Japan). The enzymes, superoxide dismutase from bovine erythrocyte and catalase from bovine liver, were also products of Wako Pure Chemicals. A Pyrex glass tube (28 mm inside diameter, 140 mm long, and 2 mm thickness) was used as a support of titanium oxide. The blacklight blue fluorescent lamp (wavelength: 300–400 nm, 6 W) was purchased from Matsushita Electronics (Tokyo, Japan) and the low-pressure mercury lamp (wavelength: 185 nm, 6 W) from Sen Special Light Source (Tokyo, Japan).

2.2. Preparation of photocatalyst and its immobilization

Amorphous titanium oxide, prepared from titanium isopropoxide according to the literature [11,12], was dissolved into an aqueous solution of hydrogen peroxide, which gave a transparent yellow solution. The inner surface of a Pyrex glass tube was covered with this viscous solution and the glass tube was calcined in a muffle furnace at 400 °C for 30 min. The same procedure was repeated five times; the fifth treatment was carried out at 500 °C for 1 h. Consequently, a transparent thin film of titanium oxide in "anatase" form was formed on the inner surface of the glass tube.

2.3. Batch-recirculation reactor system and experimental procedure

The annular-flow photocatalytic reactor consisted of a 6 W blacklight blue fluorescent lamp fixed in the center of a circular plastic vessel, a quartz glass tube to protect the lamp from being damaged by contacting with a liquid solution, and a Pyrex glass tube, whose inner surface was coated with a thin film of titanium oxide, inserted between the quartz glass tube and plastic vessel. A liquid solution was allowed to flow at a high speed through the annulus of 2 mm in width between the quartz and Pyrex glass tubes. As shown in Fig. 1, a peristaltic pump (RP-1000 type, EYELA) was used to recirculate $3.0 \times 10^{-4}\,m^3$ of the reactant solution between the photocatalytic reactor and a mixed-flow glass container at a flow rate of $6.5 \times 10^{-4}\,m^3\,min^{-1}$.

The ozone generator consisted of a $7.5 \times 10^{-4}\,m^3$ glass container in which a 6 W low-pressure mercury lamp was fixed in the center. This ozone generator was circularly connected with Teflon tubing (PTFE) to the mixed-flow glass container and an air pump (SPP-3GAS, Hiblow), as shown in Fig. 1. The oxygen contained in the air flowing through

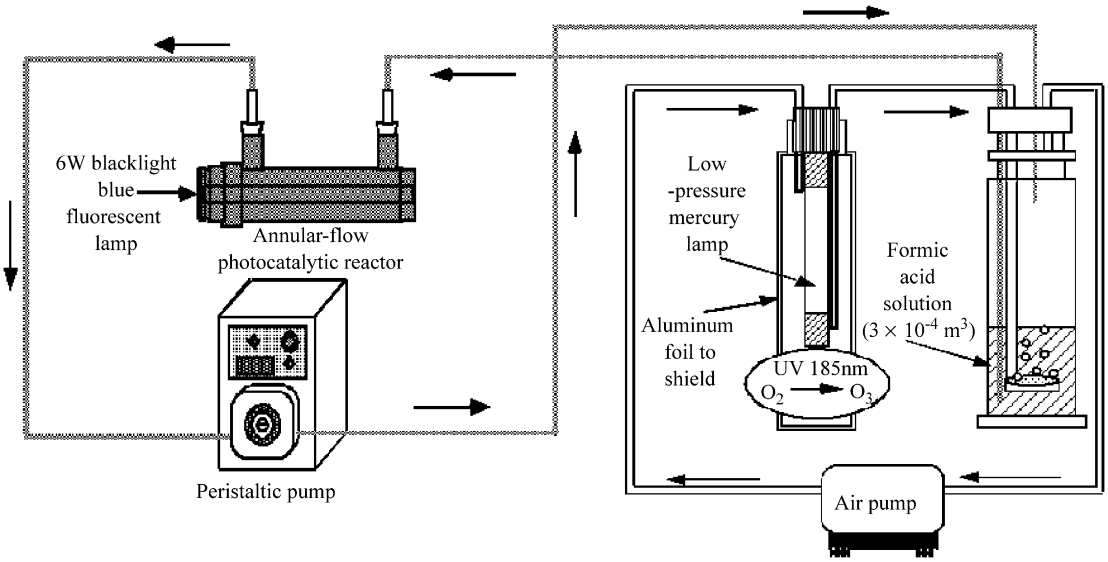

Fig. 1. Schematic of a reactor system for combined photocatalysis and ozonation in decomposition of formic acid.

the ozone generator was converted into ozone under irradiation with UV light of 185 nm in wavelength. Formic acid was decomposed when the ozone-containing air was continuously supplied to $3.0 \times 10^{-4}\,m^3$ of an aqueous formic acid solution in the mixed-flow container at a flow rate of $5.0 \times 10^{-3}\,m^3\,min^{-1}$. After circulating the air containing ozone in the reactor system for 2 min, the time course of the formic acid concentration was measured.

Three kinds of operations were carried out in a batch-recirculation manner; UV-irradiation with the blacklight blue fluorescent lamp for the photocatalysis alone, with the low-pressure mercury lamp for the ozonation alone, and with these two lamps for the combination of ozonation and photocatalysis. The initial formic acid concentration was varied in a range of 4.9–107 $g\,m^{-3}$. The whole reactor system was placed in a chamber (TRONFLI-3011NH, EYELA, Tokyo, Japan) whose inside temperature was kept at 20 °C. The liquid temperature was controlled at 20 ± 0.5 °C and the initial pH was set at 3.8 ± 0.1. Distilled water was used to prepare the formic acid solution.

The effects of free radicals on the photocatalytic decomposition of formic acid were investigated using two enzymes. The concentration of superoxide radical was reduced by the addition of superoxide dismutase in 3.0×10^8 or 5.5×10^8 units m^{-3}, where 1 unit corresponds to the amount (mg) of the enzyme required to react with 1 μmol superoxide radical within 1 min at 25 °C. On the other hand, hydrogen peroxide was decomposed by the addition of catalase in 1×10^9 units m^{-3}, where 1 unit corresponds to the amount (mg) of the enzyme required to react with 1 μmol hydrogen peroxide within 1 min at 25 °C.

The performance of the 6 W low-pressure mercury lamp to produce ozone was investigated by measuring the ozone concentration in distilled water. The effects of liquid temperature and pH on the ozonation of formic acid were further investigated. In this case, the temperature was changed in the range of 10–50 °C and the pH in the range of 2–12.

2.4. Analytical method

The formic acid concentration was determined by ion chromatography (DX-100, DIONEX). The concentrations of ozone in the air and water were determined by measuring the absorbencies of the air and water at 254 and 258 nm, respectively, with a spectrophotometer (Model 1200, Shimadzu, Tokyo, Japan) equipped with a cylindrical quartz glass cell (length: 100 mm) [13]. The concentration of inorganic carbon was determined with a TOC meter (Model 5050, Shimadzu, Tokyo, Japan).

3. Results and discussion

3.1. Photocatalytic decomposition of formic acid

Prior to the photocatalytic reaction experiment, $3.0 \times 10^{-4}\,m^3$ of an aqueous formic acid solution was recirculated over 8 h in the absence of light and little change was observed in the formic acid concentration, indicating that the adsorption of formic acid can be neglected on the wall of the reactor system including the surface of titanium oxide. Also the whole system was regarded as a perfectly mixed-flow system since the flow rate was so high ($6.5 \times 10^{-4}\,m^3\,min^{-1}$) that the conversion per one pass of the reaction mixture through the reactor was very low (less than 1%), as theoretically indicated elsewhere [14].

Fig. 2 shows the time courses of the formic acid concentration in the photocatalytic decomposition of formic acid at different initial concentrations (4.9–103 $g\,m^{-3}$). In all the cases, more than 99.5% of the formic acid was decomposed in a relatively short time. At a higher initial concentration, the formic acid was decomposed at a higher rate. It is well known that the photocatalytic reactions follow a Langmuir–Hinshelwood type [15–18]

$$r = -\frac{dC}{dt} = \frac{kK_H C}{1 + K_H C} \quad (1)$$

where r is the reaction rate, C the reactant concentration, k the kinetic constant, and K_H the adsorption equilibrium constant. When the initial decomposition rate r_0 is measured for an arbitrary initial concentration C_0, Eq. (1) can be written in a linearized form as

$$\frac{C_0}{r_0} = \frac{1}{k}C_0 + \frac{1}{kK_H} \quad (2)$$

Fig. 3 shows a plot of the initial decomposition rates determined from the experimental values in Fig. 2 against the initial formic acid concentration. From the linear relationship between C_0/r_0 and C_0, it is obvious that the photocatalytic decomposition of formic acid certainly follows the Langmuir–Hinshelwood type kinetics. From the intercept and slope of the straight line, obtained by a least-square regression, the values of k and K_H were determined to be 0.065 $g\,m^{-3}\,min^{-1}$ and 0.089 $m^3\,g^{-1}$, respectively. The solid lines in Fig. 2 show the results calculated by applying these values to Eq. (1). The calculated results are in good agreement with the experimental values obtained at the initial formic acid concentrations less than 44 $g\,m^{-3}$. When the initial concentration is 103 $g\,m^{-3}$, on the other hand, the calculated line does not agree with the experiment data except in the early stage of the reaction; it is clear that the decomposition rate for the experiment was decelerated with time compared with that for the calculation. This is considered due to the accumulation of bicarbonate ion (HCO_3^-), which is known to be a strong scavenger to the hydroxyl radical [19–21]. This reaction proceeds as

$$HCO_3^- + HO^\bullet \xrightarrow{k=1.5\times10^7\,M^{-1}\,s^{-1}} CO_3^{\bullet-} + H_2O \quad (3)$$

We also carried out the photocatalytic decomposition of formic acid at an initial concentration of 70 $g\,m^{-3}$ to estimate the bicarbonate ion concentration in the reaction mixture. When the formic acid was decomposed to 35 $g\,m^{-3}$, the dissolved inorganic carbon concentration was 1.35 $g\,m^{-3}$.

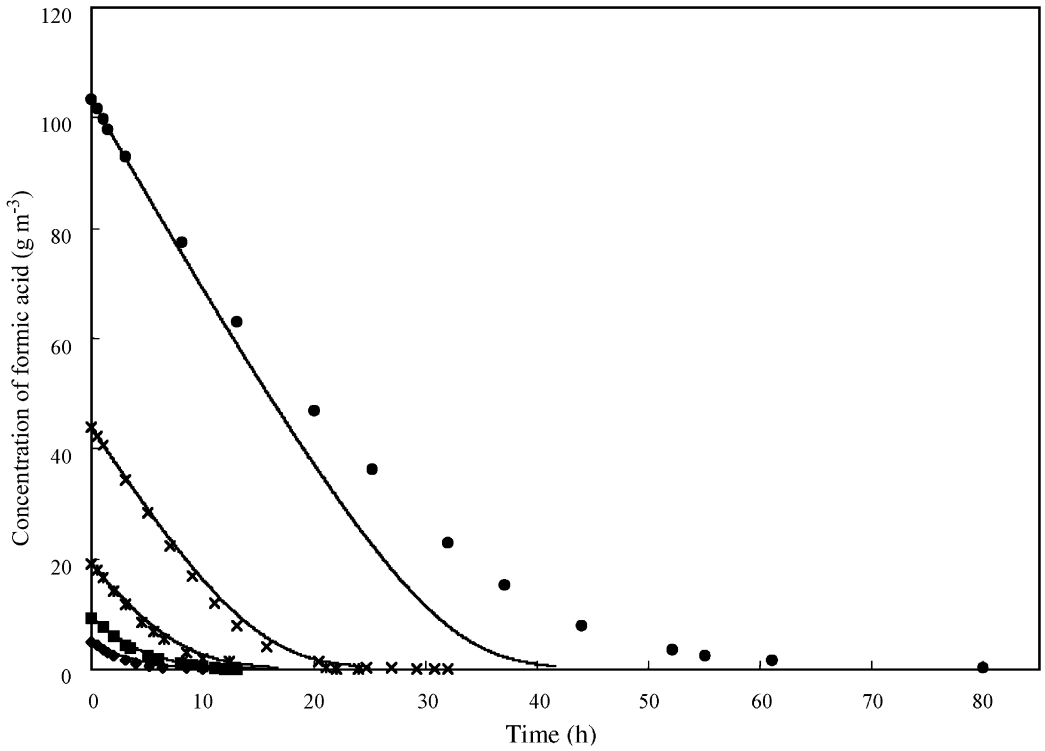

Fig. 2. Time courses of formic acid concentration in photocatalytic decomposition. The calculated line is shown by a solid line.

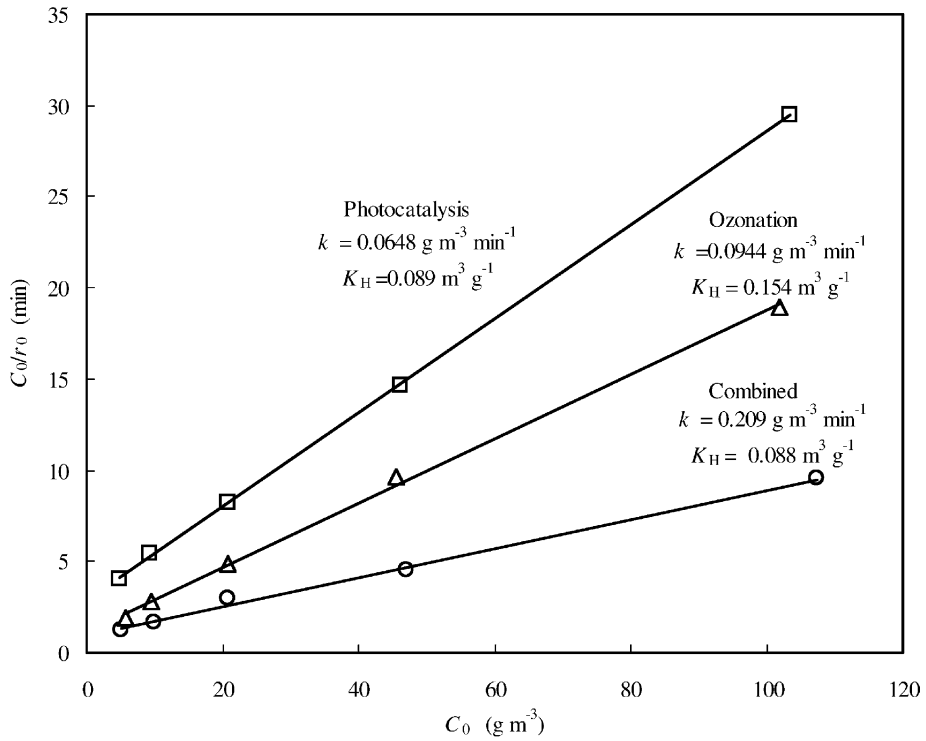

Fig. 3. Linearized plots for decompositions of formic acid by photocatalysis, ozonation, and combination of these two methods.

This value corresponds to the bicarbonate ion concentration of 6.86 g m^{-3}. At this point, the liquid pH value was 4.4; in a series of the photocatalytic decompositions of formic acid, the liquid pH value changed from 3.5–3.8 to 7.0. A further experiment was performed by adjusting the initial liquid pH to 7.0 with sodium bicarbonate, but formic acid was little decomposed. On the other hand, the surface of titanium oxide is charged positively or negatively according to the liquid pH value. The isoelectric point is present at around pH 6.3 [22]. Under an acidic condition, the surface of titanium oxide is positively charged. When the formic acid is photocatalytically decomposed, therefore, it is considered that $HCOO^-$ is easily adsorbed onto the photocatalytic surface under an acidic condition, so that the decomposition rate is increased. From these facts, we consider that a large amount of the bicarbonate ion, produced as a result of the decomposition of formic acid at a high concentration, strongly influences the photocatalytic decomposition of formic acid in the following two mechanisms:

a) Since the pH value increases with the increase of bicarbonate ion concentration, the amount of the positive charge on the photocatalytic surface decreases, so that the amount of formic acid adsorbed onto the photocatalytic surface decreases.
b) A large amount of the bicarbonate ion produced adsorbs onto the photocatalytic surface and reacts with the hydroxyl radical (Eq. (3)); thereby the hydroxyl radical concentration is decreased.

In the photocatalytic reactions, it is well known that various kinds of radicals are produced during the reaction and these are essential to the decomposition of organic compounds. At the first step, the hydroxyl and superoxide radicals including other several radicals may be produced on the surface of titanium oxide as follows:

$$TiO_2 + h\nu \rightarrow TiO_2\,(h^+_{VB} + e^-_{CB}) \quad (4)$$

$$H_2O_{(ads)} + h^+ \rightarrow HO^\bullet \quad (5)$$

$$OH^-_{(ads)} + e^- \rightarrow HO^\bullet \quad (6)$$

$$O_{2(ads)} + e^- \rightarrow O_{2(ads)}{}^{\bullet -} \quad (7)$$

$$O_{2(ads)} + e^- + H^+ \rightarrow HO_2{}^\bullet \quad (8)$$

In particular, the hydroxyl radical is indispensable to the decomposition of organic compounds. The hydroxyl radical is also generated in the ozonation, photolysis, and other oxidative treatments [17,18]. At the second step, under an acidic condition, the superoxide radical is transformed to the hydrogen peroxide according to the following mechanism [19]:

$$O_2{}^{\bullet -} + H^+ \leftrightarrow HO_2{}^\bullet \quad (9)$$

$$HO_2{}^\bullet + HO_2{}^\bullet \rightarrow H_2O_2 + O_2 \quad (10)$$

$$O_2{}^{\bullet -} + HO_2{}^\bullet \rightarrow HO_2{}^- + O_2 \quad (11)$$

$$HO_2{}^- + H^+ \rightarrow H_2O_2 \quad (12)$$

At the same time, the hydroxyl radical is produced from the superoxide radical and hydrogen peroxide as follows [19]:

$$H_2O_2 + O_2{}^{\bullet -} \rightarrow HO^\bullet + OH^- + O_2 \quad (13)$$

$$H_2O_2 \xrightarrow{h\nu} 2HO^\bullet \quad (14)$$

The hydrogen peroxide adsorbed on the surface of titanium oxide may further react with electrons and positive holes and then produce the hydroperoxyl radical as follows:

$$H_2O_{2(ads)} + e^- \rightarrow HO_2{}^\bullet + OH^- \quad (15)$$

$$H_2O_{2(ads)} + h^+ \rightarrow HO_2{}^\bullet + H^+ \quad (16)$$

To elucidate the degree of contributions of the superoxide and hydroxyl radicals to the decomposition of formic acid, the use of scavengers of these radicals is reasonable. The superoxide radical can be scavenged by superoxide dismutase (SOD), which catalyzes the following reaction:

$$2O_2{}^{\bullet -} + 2H^+ \xrightarrow{\text{superoxide dismutase}} H_2O_2 + O_2 \quad (17)$$

On the other hand, it seems difficult to find out an appropriate scavenger for the hydroxyl radical under an acidic condition. Therefore, we used catalase, which catalyzes a decomposition of hydrogen peroxide according to the following mechanism:

$$2H_2O_2 \xrightarrow{\text{catalase}} 2H_2O + O_2 \quad (18)$$

Table 1 suggests that the superoxide radical is not directly associated with the decomposition of formic acid, because there is little difference between the unconverted fractions of formic acid after 7 h with and without the addition of SOD to the solution. As seen in Fig. 4, on the other hand, the photocatalytic decomposition stopped for several hours and then started again after the catalase was deactivated. From the fact that the hydrogen peroxide produces the hydroxyl radical according to Eqs. (13) and (14), it is suggested that the hydroxyl radical as well as the hydrogen peroxide plays an important role in the decomposition of formic acid. In addition, the hydrogen peroxide may directly act on formic acid, but it was unable to prove this possibility for the present.

Table 1
Effect of SOD on photocatalytic decomposition of formic acid at an initial formic acid concentration of 20 g m^{-3}

	Control	Addition of SOD (3×10^8 units m^{-3})	Addition of SOD (5.5×10^8 units m^{-3})
Unconverted fraction of formic acid after 7 h (%)	44.3	46.4	45.4

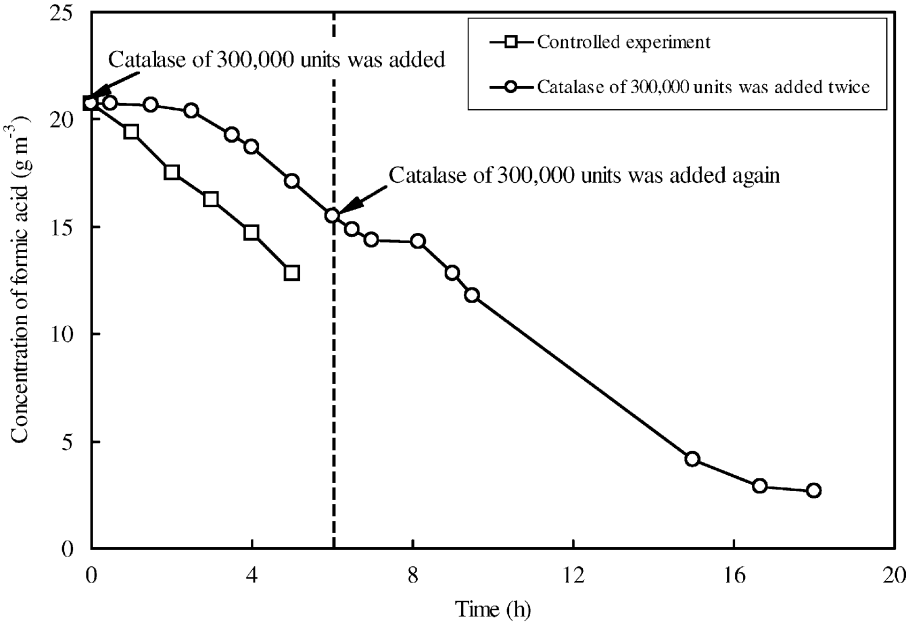

Fig. 4. Effect of hydrogen peroxide on photocatalytic decomposition of formic acid.

For the photocatalytic decomposition of formic acid, it is thus possible to consider the following reaction mechanisms [23]:

$$HO^{\bullet} + HCOOH \rightarrow HOOC^{\bullet} + H_2O_2 \quad (19)$$

$$HO^{\bullet} + HCOO^{-} \rightarrow CO_2^{\bullet -} + H_2O \quad (20)$$

$$H_2O_2 + CO_2^{\bullet -} \rightarrow HO^{\bullet} + OH^{-} + CO_2 \quad (21)$$

In this case, the hydrogen peroxide produces the hydroxyl radical and plays an indirect role to decompose formic acid.

3.2. Ozonic decomposition of formic acid

Fig. 5 shows the time courses of the ozone concentration in the air and water when the air being circulated in the closed reactor system was irradiated by UV from the low-pressure mercury lamp. The ozone concentration in the air almost linearly increased just after the lamp was turned on, rapidly reducing its production rate and reaching 162 ppmv (0.350 g m^{-3}) after 10 min. The ozone concentration in the water increased in a similar manner, although its final concentration was 0.037 g m^{-3} liquid after 30 min because of its low solubility in water. The maximum production rate of ozone in this system was estimated to be 0.960 mg min^{-1}.

Fig. 6 shows the effect of liquid temperature on the initial decomposition rate of formic acid and the ozone concentration in the water. The ozone concentration in the water decreased drastically from 0.085 to 0.002 g m^{-3} liquid with an increase of the liquid temperature from 10 to 50 °C. This can be explained by a decrease of the solubility of ozone in water and an increase of the auto-decomposition rate of ozone with an increasing liquid temperature. Similarly, the initial decomposition rate decreased markedly from 0.082 to 0.030 g m^{-3} min^{-1} for such a temperature change. It is clear that this marked decrease in the initial decomposition rate was caused by a drastic change in the ozone concentration in the water.

The concentration of hydroxyl radical produced during ozonation is affected by the liquid pH [24]. As was indicated above, moreover, the hydroxyl radical is closely associated with the decomposition of organic compounds. Therefore, the effect of initial liquid pH on the initial decomposition rate

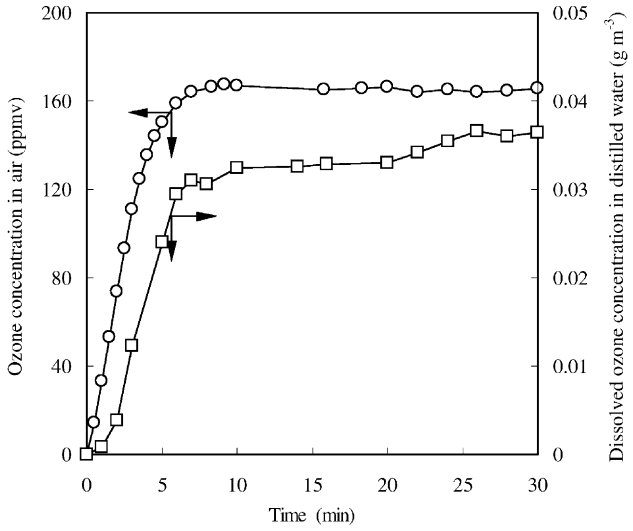

Fig. 5. Time courses of ozone concentration in air and water in an ozonation reactor.

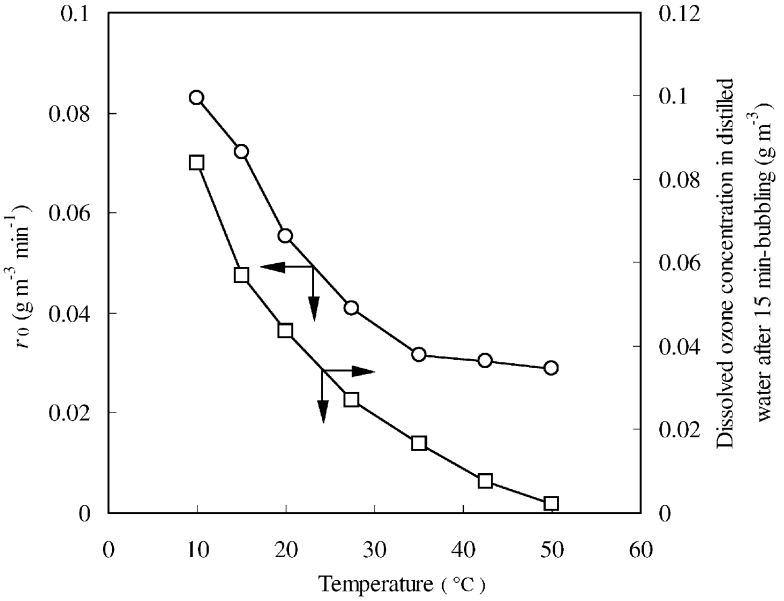

Fig. 6. Effect of temperature on initial decomposition rate of formic acid and ozone concentration in water.

of formic acid was investigated. The result is shown in Fig. 7. The larger the pH value, the higher the initial decomposition rate of formic acid. The optimal value of pH exists in the neighborhood of pH 10. This is considered due to the fact that the hydroxyl radical concentration is maintained at a high level under a high pH condition.

The mechanism of the ozonation changes according to the magnitude of the pH value [20,24]. For example, under a strongly acidic condition (pH 2), an ozone molecule directly acts on an organic compound to decompose. Under a strongly alkaline condition (pH 12), on the other hand, the ozone molecule reacts with OH^- was

$$O_3 + OH^- \rightarrow HO_2^{\bullet} + O_2^{\bullet -} \quad (22)$$

to produce intermediate radicals and finally the hydroxyl radical, which is responsible for the decomposition of organic compound.

Fig. 7 also includes the experimental data of the dissolved ozone concentration varying with pH. Under the condition of pH 10, the dissolved ozone concentration is almost zero.

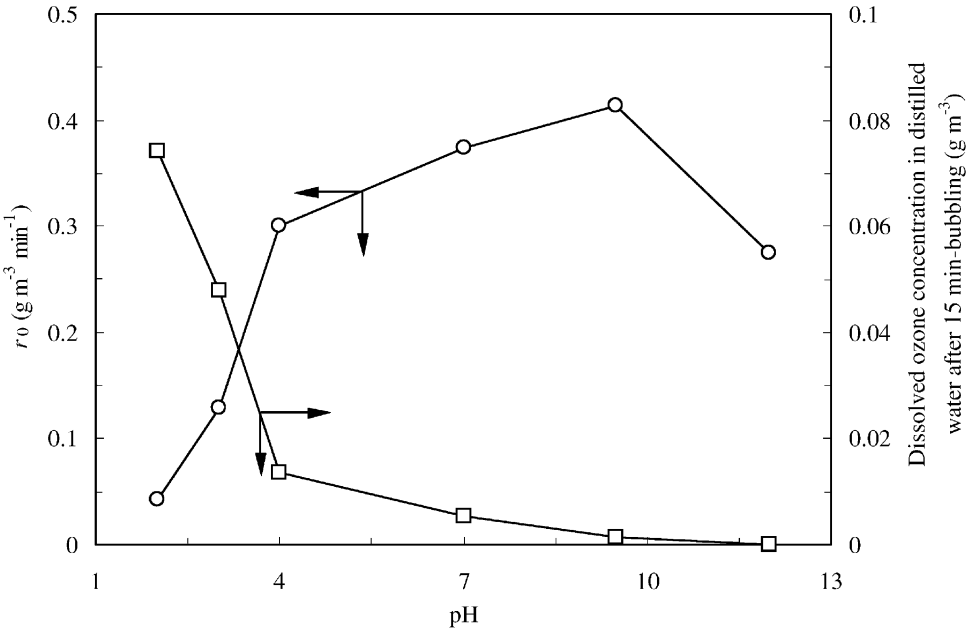

Fig. 7. Effects of pH on initial decomposition rate of formic acid and dissolved ozone concentration.

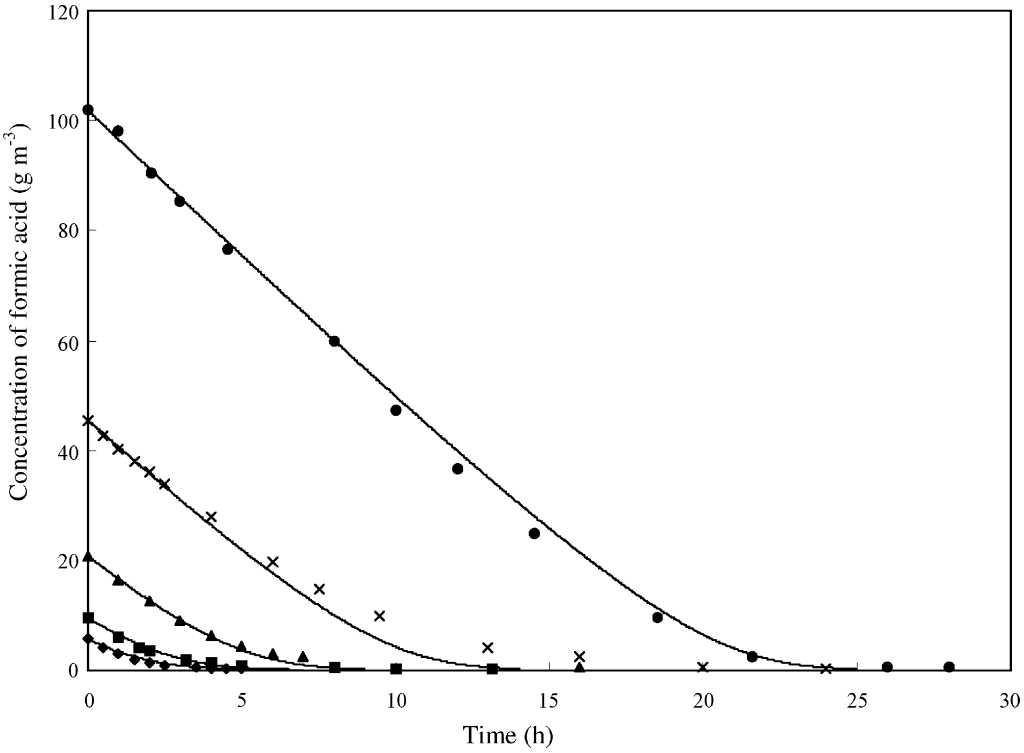

Fig. 8. Time courses of formic acid concentration in ozonic decomposition. The calculated line is shown by a solid line.

This result also indicates that under the condition of pH 10, the reactions given by Eqs. (9)–(13) and (22) are greatly responsible for the decomposition. In the ozonation under the intermediate pH condition ($2 < \text{pH} < 12$), it is considered that both the ozone molecule and hydroxyl radical are responsible for the decomposition of formic acid. That is, in the ozonation, the contribution of these chemicals to the decomposition of formic acid changes according to the magnitude of pH.

Moreover, it is reported that the kinetic constants ($k \sim 10^9\,\text{M}^{-1}\,\text{s}^{-1}$) for the reactions of hydroxyl radical with organic compounds of low-molecular-weight are significantly greater than the kinetic constants ($k = 10^{1-4}\,\text{M}^{-1}\,\text{s}^{-1}$) for the reactions of ozone with such organic compounds [4], suggesting that the ozonation proceeds more rapidly under the alkaline condition where a large amount of hydroxyl radical is produced according to Eqs. (9)–(13) and (22). Actually, our experimental result reflects this suggestion.

As described above, the photocatalytic decomposition of formic acid proceed faster under a stronger acidic condition, whereas little decomposition takes place under neutral and alkaline conditions. When the photocatalytic decomposition of formic acid is carried out together with the ozonation that was found to have the maximum decomposition rate at pH 10, therefore, it is easy to suppose that there may be an optimum pH. As shown in Fig. 7, however, there is no remarkable difference in the decomposition rates between pH 3.8 and 10. In addition, the objective of the present work was to elucidate the presence of a synergistic effect of photocatalytic reaction and ozonation on the decomposition of the formic acid that was solely dissolved in water (pH 3.8). In the present work, therefore, we did not further investigate the optimum pH.

Fig. 8 shows the time courses of the formic acid concentration in the ozonic decomposition of formic acid at different initial concentrations (5.6–102 g m^{-3}). A comparison of this experimental result with that in Fig. 2 indicates that the ozonic decomposition rate of formic acid is about two times higher than the photocatalytic decomposition rate. Like in the photocatalytic reaction, the ozonic reaction data is now kinetically analyzed. For comparison, it is convenient to introduce the same functional relationship as the Langmuir–Hinshelwood type, described as

$$r = -\frac{\mathrm{d}C}{\mathrm{d}t} = \frac{k^{\text{app}} K_{\text{H}}^{\text{app}} C}{1 + K_{\text{H}}^{\text{app}} C} \tag{23}$$

where k^{app} is the apparent kinetic constant and $K_{\text{H}}^{\text{app}}$ the apparent adsorption equilibrium constant. If the initial decomposition rate r_0 is obtained for an arbitrary initial concentration C_0, then Eq. (23) is written in a linearized form as

$$\frac{C_0}{r_0} = \frac{1}{k^{\text{app}}} C_0 + \frac{1}{k^{\text{app}} K_{\text{H}}^{\text{app}}} \tag{24}$$

The initial decomposition rates of formic acid were calculated from the experimental values in Fig. 8 for the corresponding initial formic acid concentrations and these values were plotted in the functional relationship of Eq. (24).

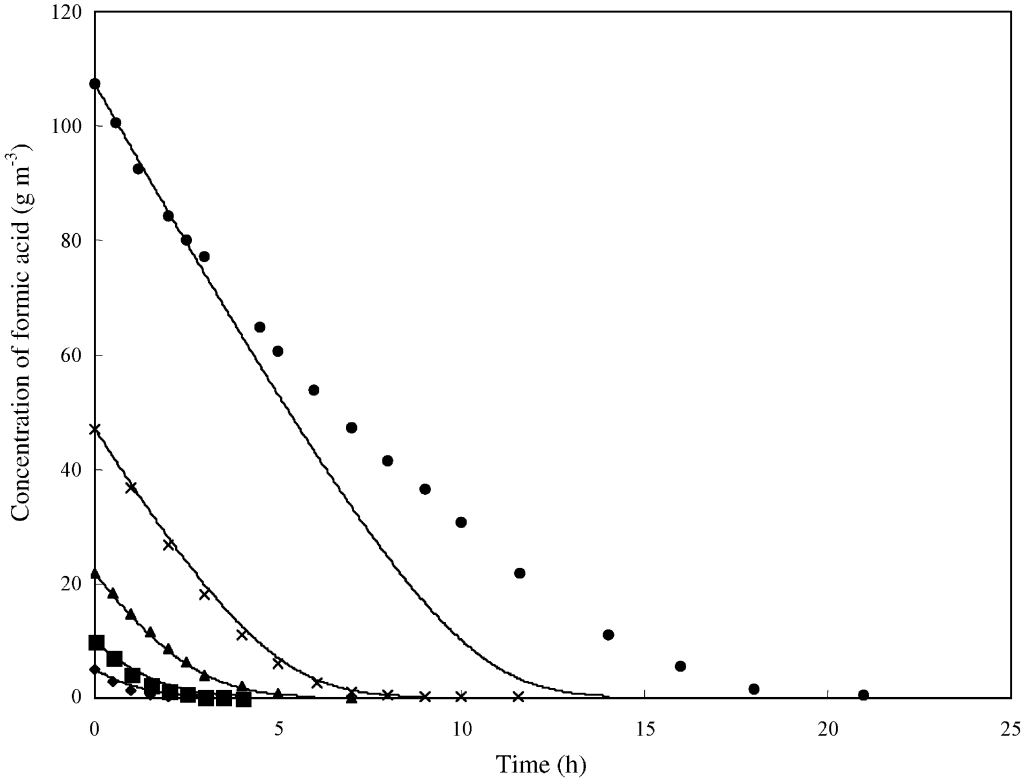

Fig. 9. Time courses of formic acid concentration in combined photocatalysis and ozonation. The calculated result is shown by a solid line.

The result is shown in Fig. 3. It is clear that there is a linear relationship between C_0/r_0 and C_0. From the slope and intercept of the straight line that was obtained by a least-square regression, the values of k^{app} and K_H^{app} were determined to be $0.094\,g\,m^{-3}\,min^{-1}$ and $0.154\,m^3\,g^{-1}$, respectively. These kinetic parameters were applied to Eq. (23) and the time courses of the formic acid concentration were calculated. The results are shown by solid lines in Fig. 8. The calculated lines are in good agreement with the experimental values for all the runs.

3.3. Decomposition of formic acid by combination of photocatalysis and ozonation

Fig. 9 shows the time courses of the formic acid concentration in the simultaneous photocatalytic and ozonic decompositions of formic acid at different initial concentrations (5.0–$107\,g\,m^{-3}$). It is clear that the formic acid was rapidly decomposed by the combination of these two methods compared to the decomposition by the photocatalysis or ozonation alone. The initial decomposition rates were calculated from the experimental values in Fig. 9 and these values were plotted in a linearized form given by Eq. (24). The result is shown in Fig. 3. From the slope and intercept of the straight line that was obtained by a least-square regression, the values of k^{app} and K_H^{app} were determined to be $0.209\,g\,m^{-3}\,min^{-1}$ and $0.088\,m^3\,g^{-1}$, respectively. The solid lines in Fig. 9 show calculated lines by integration of Eq. (23). The calculated results are in good agreement with the experimental values for the initial formic acid concentrations less than $47.1\,g\,m^{-3}$. At the initial concentration of $107\,g\,m^{-3}$, on the other hand, the calculated line does not agree with the experiment data except in the early stage of the reaction. Like the case of the photocatalysis alone, this is considered due to the accumulation of bicarbonate that acted as a scavenger for the hydroxyl radical [19,20].

3.4. Comparisons of the decompositions of formic acid by three methods

Table 2 summarizes the kinetic parameters determined in the decompositions of formic acid by the three methods, i.e., photocatalysis, ozonation, and combination of these methods. A comparison indicates that the kinetic constant for the combination of photocatalysis and ozonation is 31% larger than the sum of those for the photocatalysis and ozonation; in other words, the decomposition rate for the combination of photocatalysis and ozonation is 31% higher at maximum than the sum of those for the photocatalysis and ozonation. The kinetic parameters for the three methods were used to calculate the relationship between r and C using Eq. (1) or (23). The results are shown in Fig. 10. It is clear that over the entire range of formic acid concentration, the decomposition rate of formic acid by the combination of photocatalysis and ozonation is larger than the sum of those by each of the two methods. These results clearly indicate

Table 2
Comparison of kinetic parameters determined in decompositions of formic acid by different methods

	Photocatalysis	Ozonation	Combination of photocatalysis and ozonation
k or k^{app} ($g\,m^{-3}\,min^{-1}$)	0.0648	0.0944	0.209
K_H or K_H^{app} ($m^3\,g^{-1}$)	0.089	0.154	0.088

that a synergistic effect appears when the photocatalytic and ozonic treatments are performed simultaneously. This effect may be based on the increase in the concentrations of reactive intermediates, such as hydrogen peroxide, hydroxyl radical, and so on, produced by the ozone dissolving in an aqueous formic acid solution flowing through the photocatalytic reactor. The following two reasons are considered for the facilitated production of the intermediate radicals.

Firstly, it is considered that in the photocatalytic reactor, the dissolved ozone was easy to get electrons produced on the surface of titanium dioxide according to the mechanism

$$O_{3(ads)} + e^- \rightarrow O_{3(ads)}{}^- \quad (25)$$

so that recombination of the positive holes with the electrons was interfered. Consequently, a larger number of radicals were produced, thereby accelerating the photocatalytic reaction. There are other examples in which the photocatalytic decompositions of organic compounds were accelerated by the addition of oxidizers. Pelizzetti et al. [25] have found that the photocatalytic decompositions of 2-chlorophenol, 2,7-dichlorodibenzodioxin, and atrazine can be improved by the addition of $K_2S_2O_8$ and KIO_4.

Secondly, it is considered that a larger number of hydrogen peroxide and hydroxyl radicals were produced from the dissolved ozone as a result of UV-irradiation or getting electrons on the photocatalyst surface [26]. For example, when the dissolved ozone is irradiated by UV light (<310 nm) in an ozonic oxidation process, a contribution of the radical reactions to the ozonation is increased, which makes it possible, in turn, to treat organic compounds that are impossible to degrade by ozone alone [2,25,26]. Under an acidic condition, moreover, it has been reported that in the ozonation under UV-irradiation, the hydroxyl radical is produced according to the following mechanism [27–29]:

$$O_3 + H_2O \xrightarrow{h\nu} H_2O_2 + O_2 \quad (26)$$

$$H_2O_2 \xrightarrow{h\nu} 2HO^\bullet \quad (27)$$

$$H_2O_2 \leftrightarrow HO_2{}^- + H^+ \quad (28)$$

$$O_3 + HO_2{}^- \rightarrow O_3{}^{\bullet -} + HO_2{}^\bullet \quad (29)$$

$$HO_2{}^\bullet \rightarrow O_2{}^{\bullet -} + H^+ \quad (30)$$

$$O_3 + O_2{}^{\bullet -} \rightarrow O_3{}^{\bullet -} + O_2 \quad (31)$$

$$O_3{}^{\bullet -} + H^+ \leftrightarrow HO_3{}^\bullet \quad (32)$$

In conclusion, it is considered that the decomposition of formic acid was facilitated by a synergistic effect of photocatalysis and ozonation.

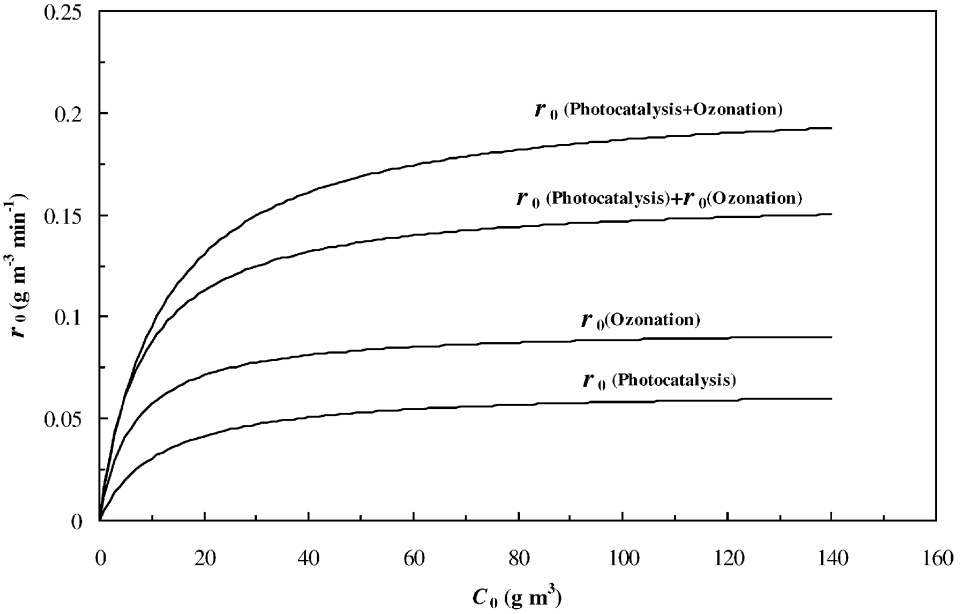

Fig. 10. Comparisons among calculated results for a relationship between decomposition rate and formic acid concentration in photocatalysis, ozonation, and combination of these two methods.

4. Conclusions

The decompositions of formic acid at the initial concentrations of 4.9–107 $g\,m^{-3}$ by three different methods (photocatalysis with a 6 W blacklight blue fluorescent lamp, ozonation with a 6 W low-pressure mercury lamp, and combination of these methods) were studied. As a result, the following conclusions were withdrawn:

1) The photocatalytic decomposition of formic acid follows Langmuir–Hinshelwood type kinetics.
2) The hydroxyl radical and hydrogen peroxide produced as a result of the photocatalytic reaction have a great effect on the decomposition of formic acid, whereas the superoxide radical has little effect.
3) In the reactor system investigated here, the ozone concentrations in the air and water reached 0.350 $g\,m^{-3}$ air and 0.037 $g\,m^{-3}$ liquid, respectively, and the formic acid was rapidly decomposed. This time-transient behavior is conveniently expressed in the form of Langmuir–Hinshelwood type.
4) The decomposition rate of formic acid becomes faster under the conditions of a lower liquid temperature and higher pH. The optimal pH value exists in the neighborhood of pH 10.
5) The decomposition rate of formic acid is increased by 31% at maximum as a result of the combination of photocatalysis and ozonation, compared with treatments by their respective methods. This increase is considered due to the synergistic effect of photocatalysis and ozonation.
6) Two possible mechanisms are considered for the synergistic effect; a recombination of electrons and positive holes interfered by the reaction between ozone and electrons on the surface of titanium oxide and a production of hydrogen peroxide increased by UV-irradiation of ozone.

References

[1] S.-J. Kim, K.-H. Oh, S.-H. Lee, S.-S. Choi, K.-C. Lee, Study on secondary reaction and fate of hazardous chemicals by oxidants, Water Sci. Technol. 36 (1997) 325.

[2] S. Echigo, H. Yamada, S. Matsui, S. Kawanishi, K. Shishida, Comparison between O_3/VUV, O_3/H_2O_2, VUV and O_3 processes for the decomposition of organophosphoric acid triesters, Water Sci. Technol. 34 (1996) 81.

[3] S.D. Lambert, N.J.D. Graham, Removal of non-specific dissolved organic matter from upland potable water supplies: II. Ozonation and adsorption, Water Res. 29 (1995) 2427.

[4] V. Camel, A. Bermond, The use of ozone and associated oxidation processes in drinking water treatment, Water Res. 32 (1998) 3208.

[5] J.Y. Hu, Z.S. Wang, W.J. Ng, S.L. Ong, The effect of water treatment processes on the biological stability of potable water, Water Res. 33 (1999) 2587.

[6] J.D. Plummer, J.K. Edzwald, Effect of ozone on disinfection by-product formation of algae, Water Sci. Technol. 37 (1998) 49.

[7] A. Hirvonen, T. Tuhkanen, P. Kalliokoski, Treatment of TCE- and PCE-contaminated groundwater using UV/H_2O_2 and O_3/H_2O_2 oxidation processes, Water Sci. Technol. 33 (1996) 67.

[8] J.C. Crittenden, J. Liu, D.W. Hand, D.L. Perram, Photocatalytic oxidation of chlorinated hydrocarbons in water, Water Res. 31 (1997) 429.

[9] R.P.S. Suri, J. Liu, D.W. Hand, J.C. Crittenden, D.L. Perram, M.E. Mullins, Heterogeneous photocatalytic oxidation of hazardous organic contaminants in water, Water Environ. Res. 65 (1993) 665.

[10] L. Sanchez, J. Peral, X. Domenech, Aniline degradation by combined photocatalysis and ozonation, Appl. Catal. B 19 (1998) 59.

[11] K. Matsuo, T. Takeshita, K. Nakano, Formation of thin films by the treatment of amorphous titania with H_2O_2, J. Cryst. Growth 99 (1990) 621.

[12] F. Shiraishi, K. Toyoda, S. Fukinbara, E. Obuchi, K. Nakano, Photolytic and photocatalytic treatment of an aqueous solution containing microbial cells and organic compounds in an annular-flow reactor, Chem. Eng. Sci. 54 (1999) 1547.

[13] Standard Methods for the Examination of Water and Wastewater, APHA-AWWA-WPCF, Washington, DC, 1989.

[14] S. Fukinbara, F. Shiraishi, K. Nagasue, A mathematical model for batch-recirculation reactor systems and its numerical calculation method, CELSS J. 12 (2000) 9.

[15] C. Kormann, D.W. Bahnemann, M.R. Hoffmann, Photolysis of chloroform and other organic molecules in aqueous TiO_2 suspensions, Environ. Sci. Technol. 25 (1991) 494.

[16] D.F. Ollis, C.-Y. Hsiao, L. Budiman, C.-L. Lee, Heterogeneous photoassisted catalysis: conversions of perchloroethylene, dichloroethane, chloroacetic acids and chlorobenzenes, J. Catal. 88 (1984) 89.

[17] R.W. Matthews, Purification of water with near-UV illuminated suspensions of titanium dioxide, Water Res. 24 (1990) 653.

[18] C.S. Turchi, D.F. Ollis, Photocatalytic degradation of organic water contaminants: mechanisms involving hydroxyl radical attack, J. Catal. 122 (1990) 178.

[19] D.D. Dionysiou, M.T. Suidan, E. Bekou, I. Baudin, J.-M. Lainek, Effect of ionic strength and hydrogen peroxide on the photocatalytic degradation of 4-chlorobenzoic acid in water, App. Catal. B 26 (2000) 153.

[20] G.V. Buxton, C.L. Greenstock, W.P. Helman, A.B. Ross, Critical review of rate constants for reactions of hydrated electrons, hydrogen atoms and hydroxyl radicals ($^{\bullet}OH/O^{\bullet -}$) in aqueous solution, J. Phys. Chem. Ref. Data 17 (1988) 513.

[21] J.L. Weeks, J. Rabani, The pulse radiolysis of deaerated carbonate solutions. I. Transient optical spectrum and mechanism. II. p*K* for OH radicals, J. Phys. Chem. 82 (1966) 138.

[22] G.A. Parks, The isoelectric points of solid oxides, solid hydroxides, and aqueous hydroxy complex systems, Chem. Rev. 65 (1965) 177.

[23] V. Karpel, N. Leitner, M. Dore, Hydroxyl radical induced decomposition of aliphatic acids in oxygenated and deoxygenated aqueous solutions, J. Photochem. Photobiol. A 99 (1996) 137.

[24] J. Hoigne, The chemistry of ozone in water, in: S. Stucki, Process Technologies for Water Treatment, Vol. 121, Plenum Press, New York, 1988.

[25] E. Pelizzetti, V. Carlin, C. Minero, M. Gratzel, Enhancement of the rate of photocatalytic degradation on TiO_2 of 2-chlorophenol, 2,7-dichlorodibenzodioxin and atrazine by inorganic oxidizing species, New J. Chem. 15 (1991) 351.

[26] V. Beschkkov, G. Bardarska, H. Gulyas, I. Sekoulov, Degradation of triethylene glycol dimethyl ether by ozonation combined with UV irradiation or hydrogen peroxide addition, Water Sci. Technol. 36 (1997) 131.

[27] D.G. Mirat, R. Vatistas, Oxidation of phenolic compounds by ozone and ozone/UV radiation: a comparative study, Water Res. 21 (1988) 895.

[28] G.R. Peyton, W.H. Glaze, Destruction of pollutants in water with ozone in combination with ultraviolet radiation. Part 3. Photolysis of aqueous ozone, Environ. Sci. Technol. 22 (1988) 761.

[29] R. Andreozzi, V. Caprio, A. Insola, R. Marotta, Advanced oxidation process (AOP) for water purification and recovery, Catal. Today 53 (1999) 51.